lations presented earlier. In comparison to the results in Table VIII, the multireference calculation of Sloan et al.[23] orders the states slightly differently: $^3\Pi$, $^3\Sigma$, $^1\Delta$, $^1\Pi$. Further the RMOS fitted surface yields a $^3\Pi$–$^1\Delta$ separation at the anion geometry of only 0.63 eV. Apparently, all four surfaces should be considered before assigning all of the experimental spectrum's features. In addition, the inclusion of the spin–orbit interaction will result in even more potential energy surfaces to be considered.

Summary

We have shown that the photoelectron experiment successfully probes the transition state of an asymmetric triatomic hydrogen abstraction reaction, namely, the F + OH reaction. The nature of the system, where all atoms are first row and consequently few electrons are involved, makes it amenable to a high-level ab initio potential surface characterization. We hope the results presented here will stimulate such theoretical interest. The photoelectron spectra of CH_3OHF^- and $C_2H_5OHF^-$ have demonstrated the extension of our method to polyatomic reactions and have shown that vibrational structure at the transition state can still be resolved even when the transition species has 10 atoms. The interpretation of our spectra is relatively simple at a qualitative level and mirrors the work on the bihalide systems. A simulation that explicitly treats the collinear dynamics of F + OH, using a multireference ab initio potential surface, has been performed and yields reasonable agreement with the experimental result.

However, a detailed understanding of the spectra is clouded by a number of difficult theoretical questions. The simulation for the F + OH system assumes that the transition state is collinear and ignores the effect of the bending degree of freedom on the dissociation dynamics and, thus, on the photoelectron spectra. Schatz[77] has reviewed the theoretical formalism of photodetachment to the transition state of a bimolecular reaction in three dimensions. Schatz has also compared the results of exact collinear treatments, like this one, with three-dimensional $J = 0$ coupled

channel hyperspherical (CCH) simulations for the $ClHCl^-$ and IHI^- photoelectron spectra. He finds good agreement in the qualitative features. For the bihalide systems, the assumption of a collinear transition state is more reasonable than it is here. There is considerable evidence[78] that the $O(^3P)$ + HCl → OH + Cl reaction proceeds via a bent transition state; Gordon et al.[79] have calculated the saddle point geometry and find $\angle OHCl = 138°$. The question then arises whether the collinear $^3\Pi$ interaction $O(^3P)$ + HF is also unstable with respect to bending and whether a bent transition state is preferred for this reaction also. However, a major difference between the two reactions is that O + HCl is approximately thermoneutral whereas O + HF is endogeric by 34 kcal/mol.

The similarity in the OHF^-, CH_3OHF^-, and $C_2H_5OHF^-$ spectra indicates that the pseudotriatomic model fairly successfully describes the polyatomic systems' spectra. However, development of theoretical methods of treating polyatomic reaction systems is clearly desirable. Further experiments from this laboratory will be forthcoming on transition-state spectra for tetraatomic systems, the results of which should be able to test theoretical methods for such systems.

(77) Schatz, G. C. *J. Phys. Chem.* **1990**, *94*, 6157.

(78) Rakestraw, D. J.; McKendrick, K. G.; Zare, R. N. *J. Chem. Phys.* **1987**, *87*, 7341.

(79) Gordon, M. S.; Baldridge, K. K.; Bernholdt, D. E.; Bartlett, R. J. *Chem. Phys. Lett.* **1989**, *158*, 189.

Translational Energy Distribution from C_2H_2 + $h\nu$(193.3 nm) → C_2H + H[†]

J. Segall, Y. Wen, R. Lavi,[‡] R. Singer, and C. Wittig*

Department of Chemistry, University of Southern California, Los Angeles, California 90089-0482 (Received: March 26, 1991)

We report the center-of-mass translational energy distribution for 193.3-nm photolysis of expansion-cooled C_2H_2, using high-n Rydberg-level excitation of nascent H atoms to facilitate high-resolution time-of-flight measurements. The observed resolution of ~200 cm⁻¹ is presently limited by the ArF photolysis laser, whose band width is approximately 200 cm⁻¹. The reported distribution clearly resolves a C_2H bending progression (ν_2 ~ 400 cm⁻¹), which reflects the trans-bent C_2H_2 excited state. A definitive assignment of all features is still not possible on the basis of currently available information on C_2H. These measurements yield an upper bound to D_0 of 131.8 ± 0.5 kcal mol⁻¹.

Introduction

The spectroscopy and photochemistry of acetylene have been studied extensively, both experimentally[1–8] and theoretically.[9] Early spectroscopic investigations showed a prominent bending progression in the $\tilde{A}^1A_u \leftarrow \tilde{X}^1\Sigma_g^+$ absorption spectrum, indicating that the first electronically excited state is trans bent.[1,2] Photochemical studies showed that photolysis at wavelengths shorter than ~200 nm yields the ethynyl radical, C_2H, and an H atom.[3] Wodtke and Lee reported the center-of-mass (CM) translational

energy distribution following 193.3-nm photolysis using the angle-resolved time-of-flight (TOF) method, and gave an upper

(1) Innes, K. K. *J. Chem. Phys.* **1955**, *22*, 863.

(2) Innes, K. K. *J. Chem. Phys.* **1955**, *22*, 863.

(3) Irion, M. P.; Kompa, K. L. *Appl. Phys.* **1982**, *B27*, 183.

(4) Wodtke, A. M.; Lee, Y. T. *J. Phys. Chem.* **1985**, *89*, 4744.

(5) Ervin, K. M.; Gronert, S.; Barlow, S. E.; Gilles, M. K.; Harrison, A. G.; Bierbaum, V. M.; DePuy, C. H.; Lineburger, W. E.; Elisson, G. B. *J. Am. Chem. Soc.* **1990**, *112*, 5750.

(6) Baldwin, D. P.; Buntine, M. A.; Chandler, D. W. *J. Chem. Phys.* **1990**, *93*, 6578.

(7) Segall, J.; Lavi, R.; Wen, Y.; Wittig, C. *J. Phys. Chem.* **1989**, *93*, 7287.

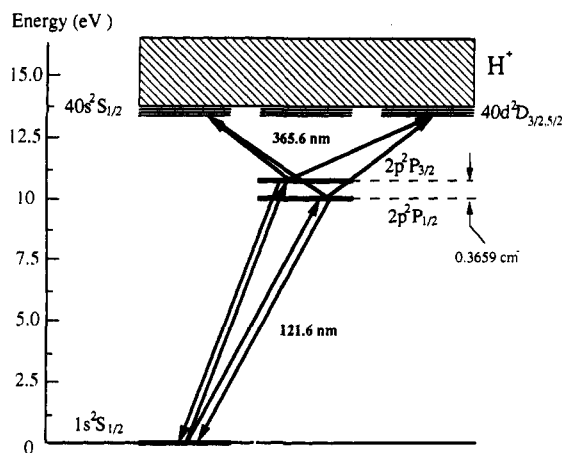(8) Green, P. G.; Kinsey, J. L.; Field, R. W. *J. Chem. Phys.* **1989**, *91*, 5160.

Figure 1. Excitation scheme for the detection of H atoms via high-lying Rydberg levels.

bound to the dissociation energy of $D_0(C_2H-H) = 132 \pm 2$ kcal mol^{-1}.[4] Yet important questions remain. In particular, $D_0(C_2$-H-H) has remained the focus of experimental and theoretical study, and the fragmentation dynamics of the excited C_2H_2 reactive precursor are essentially unknown. Most recent studies have yielded upper limits for D_0 around 131 kcal mol^{-1},[5,6] while values around 127 kcal mol^{-1} have also been reported.[7,8]

Likewise, the ethynyl radical has also been a fertile area for study. C_2H was first observed in interstellar media in 1974[10] and plays an important role in combustion and in the formation of soot.[11] It has been investigated by ESR,[12,13] infrared and visible spectroscopies[14,15] in rare-gas matrices, and by LMR,[16] emission,[17] microwave,[18] color center,[19-21] and diode laser[22,23] spectroscopies in the gas phase. Of particular relevance to the work reported here, Fletcher and Leone observed IR emission in the region 3600–4100 cm^{-1} from C_2H created by 193-nm C_2H_2 photolysis.[17] In addition, extensive theoretical efforts have followed.[24,25] However, as with C_2H_2, many important physical properties of C_2H remain elusive. While both theory[24] and experiment[17,19-21] point to the presence of a low-lying electronic state ~3500–4000 cm^{-1} above the ground state, assignment of the $\tilde{A}^2\Pi$ origin has been the subject of controversy.[20,21] In addition, the ν_1 CH stretch has not been reliably assigned, and the ν_2 bend has not been observed directly, although Hirota and co-workers derive a ν_2 frequency of 372 cm^{-1} from their observation of combination and hot-band transitions.[22] The ν_3 CC stretch was first observed in low-temperature matrices by Jacox[14] and in the gas phase at 1841
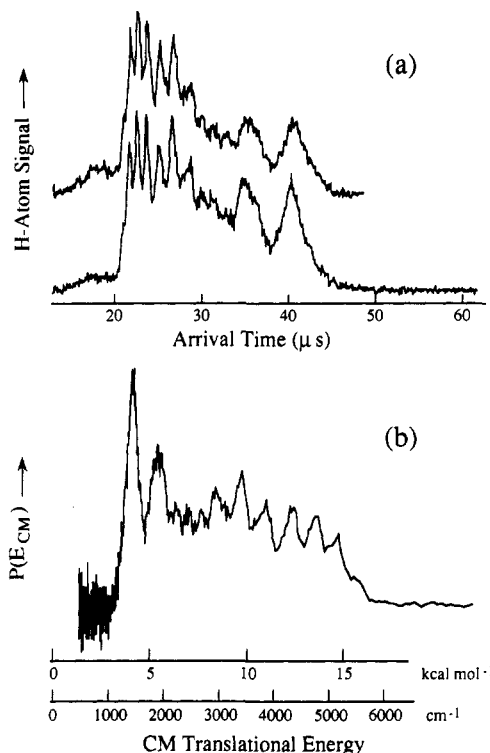

Figure 2. (a) H-atom TOF spectra, obtained using a 23.6-cm flight path (offset by an arbitrary amount). (b) Data from the upper TOF spectrum transformed to a CM translational energy scale.

cm^{-1} by Kanamori and Hirota.[22]

In this article, we report the $C_2H_2 + h\nu \rightarrow H + C_2H$ center-of-mass translational energy distribution for 193.3-nm photolysis, at higher resolution (i.e., ~200 cm^{-1}) than has been reported previously. The present results are the first to clearly resolve the ν_2 C_2H bending progression that dominates the distribution. The Rydberg TOF method employed offers the possibility of high translational energy resolution (i.e., tens of cm^{-1}), which may ultimately be needed to establish D_0 beyond reasonable doubt. Although we cannot yet assign all of the observed spectral features, the present results offer insight into the photophysics of C_2H_2 photodissociation, as well as the physical properties of the ethynyl radical.

Experimental Section

The technique of detecting H atoms via 2-photon, 2-frequency excitation to a high-lying Rydberg state followed by efficient field ionization at the desired detection region was proposed by Letokhov[26] and developed by Welge and co-workers.[27] The principles are shown schematically in Figure 1. Briefly, a supersonic expansion of C_2H_2 seeded in He is skimmed and crossed with a portion of the output from an ArF excimer laser, which is weakly focused by using a 1-m lens. H-atom fragments are excited by VUV light tuned to the line center of the Lyman α transition at 121.6 nm. The Lyman α radiation is generated by tripling the output of an excimer laser-pumped dye laser (364.7 nm) in Kr.[28] Another excimer laser-pumped dye laser beam, overlapping the 121.6-nm beam, transfers H-atom population from the 2^2P level to a high-lying Ryberg level (e.g., $n = 40$–90). In contrast to the rapidly fluorescing 2^2P state, high-n Rydberg levels are radiatively metastable and remain highly excited for many tens of microseconds. These excited atoms travel to a detector 23.6 cm from the interaction region, with Doppler selection in the Lyman α step

(9) Curtiss, L. A.; Pople, J. A. *J. Chem. Phys.* **1989**, *91*, 2420 and references therein.
(10) Tucker, K. D.; Kutner, M. L.; Thaddeus, P. *Astrophys. J.* **1974**, *193*, L115.
(11) Miller, J. H.; Hamins, A.; Kohout, T. A.; Smyth, K. C.; Mallard, W. G. *Am. Chem. Soc., Div. Fuel Chem., Prepr.* **1987**, *32*, 505.
(12) Cochran, E. L.; Adrian, F. J.; Bowers, V. A. *J. Chem. Phys.* **1964**, *40*, 213.
(13) Graham, W. R. M.; Dismuke, K. I.; Weltner, W. *J. Chem. Phys.* **1974**, *60*, 3817.
(14) Jacox, M. E. *Chem. Phys.* **1975**, *7*, 424.
(15) Jacox, M. E.; Olson, W. B. *J. Chem. Phys.* **1987**, *86*, 3134.
(16) Saykally, R. J.; Veseth, L.; Evenson, K. M. *J. Chem. Phys.* **1984**, *80*, 2247.
(17) Fletcher, T. R.; Leone, S. R. *J. Chem. Phys.* **1989**, *90*, 871.
(18) Bogey, M.; Demuynck, C.; Destombes, J. L. *Astron. Astrophys.* **1985**, *144*, L15.
(19) Curl, R. F.; Carrick, P. J.; Merrer, A. J. *J. Chem. Phys.* **1985**, *82*, 3479; *J. Chem. Phys.* **1985**, *83*, 4278.
(20) Yan, W.; Dane, C. B.; Zietz, D.; Hall, J. L.; Curl, R. F. *J. Mol. Spectrosc.* **1987**, *123*, 486.
(21) Yan, W.; Warner, H. E.; Amano, T. *J. Chem. Phys.* **1991**, *94*, 1712.
(22) Kanamori, H.; Hirota, E. *J. Chem. Phys.* **1988**, *89*, 3962.
(23) Kanamori, H.; Seki, K.; Hirota, E. *J. Chem. Phys.* **1987**, *87*, 73.
(24) Koures, A.; Harding, L. B. *J. Phys. Chem.* **1991**, *95*, 1035 and references therein.
(25) Bauschlicher, C. W., Jr.; Langhoff, S. R. *Chem. Phys. Lett.* **1990**, *173*, 367 and references therein.

(26) Letokhov, V. S. In *Chemical and Biochemical Applications of Lasers*; Moore, C. B., Ed. Academic Press: New York, 1980; Vol. V.
(27) Schnieder, L.; Meier, W.; Welge, K. H.; Ashfold, M. N. R.; Western, C. M. *J. Chem. Phys.* **1990**, *92*, 7027.
(28) Zacharias, H.; Rottke, H.; Danon, J.; Welge, K. H. *Opt. Commun.* **1981**, *37*, 15.

ensuring that the largest possible fraction of excited H atoms are sent toward the detector. Since the excited atoms are neutral, they are not affected by stray fields and space charge. The latter is a major problem when detecting proton TOF following laser ionization in the photodissociation region.[27] Once the excited H atoms arrive at the detector, they are easily field-ionized and are then detected as ions. TOF spectra are recorded by using a transient digitizer and a computer.

Results and Discussion

Figure 2a shows two TOF spectra. Although relative intensities differ slightly for the two traces, the main features are very reproducible: a small unstructured contribution at 15–20 μs, followed by a series of well-resolved peaks. The 15–20-μs feature will be discussed below. Figure 2b shows the structured region of the upper TOF spectrum transformed (including Jacobian) to a CM translational energy scale. Contributions from the beam velocity are minimal due to high C_2H_2/He ratios and correspondingly low beam velocities ($\sim 10^5$ cm s^{-1}). Since the CM translational energy distribution mirrors the C_2H internal energy distribution, it is evident that C_2H is highly excited. These results agree qualitatively with the distribution reported by Wodtke and Lee,[4] but the present measurements reveal considerably more detail. In particular, there is a striking progression of features between 3000 and 5500 cm^{-1}, spaced ~ 410 cm^{-1} apart. Since only the ν_2 bending mode of C_2H has a frequency near this value, these peaks clearly form a bending progression. This is not surprising, since the equilibrium geometry of the predissociating C_2H_2 A state is trans bent, whereas the equilibrium geometry of C_2H is linear in both the $\tilde{X}^2\Sigma$ and $\tilde{A}^2\Pi$ states. Between 2000 and 3000 cm^{-1}, there are three closely spaced, yet resolved, peaks, followed by the two most prominent features in the spectrum. No signal is observed below ~ 1000 cm^{-1}.

Our tentative assignment for the 15–20-μs signal is C_2H photolysis:

$$C_2H + h\nu(193.3 \text{ nm}) \rightarrow C_2 + H \qquad (1)$$

This is known to occur in 193.3-nm C_2H_2 photolysis and has been studied recently by Jackson and co-workers.[29] Although this could, in principle, result in a structured spectrum, it seems likely that several different C_2H vibrational levels will absorb photolysis radiation and dissociate, resulting in a relatively structureless spectrum. It is possible that this contribution to the TOF spectrum is responsible for the signal observed in the wings of Doppler spectra.[7] Preliminary results indicate that the 15–20-μs signal has a similar photolysis fluence dependence to that of the main signal, in agreement with that reported in the Doppler work; this is consistent with the C_2H absorption cross section being much higher than that of C_2H_2 photolysis. If C_2H photolysis is responsible for the 15–20-μs signal, it is likely that the signal persists at longer arrival times and the structured part of the TOF spectrum from 20 to 40 μs lies on top of an unstructured background. Another explanation is that the 10–15-μs signal results from a small number of highly excited hydrogen atoms that are field ionized in the TOF tube.

To better understand the results, we simulated the observed distribution by convoluting a "stick spectrum" with the measured experimental resolution. Photodissociation experiments with HBr and HI at 193 and 248 nm showed that the C_2H_2 experimental resolution is given by the band width of the ArF photolysis laser, $\Delta E_{fwhm} \sim 200$ cm^{-1}. The feature in the experimental spectrum around 3000 cm^{-1} appears to be a doublet, and is thus simulated by using two lines. The other peaks are better resolved. The stick spectrum and its convolution that best fits the data are shown in Figure 3a, and the results are summarized in Table I. For purposes of discussion, the 13 resolved features are labelled a–m. Peaks g–k and peak m are well reproduced in the simulation, but the simulated peaks l and a–f are narrower than the data. Closer inspection of the data shows that peaks a–f appear to degrade toward lower energies, suggesting rotational excitation. Conse-
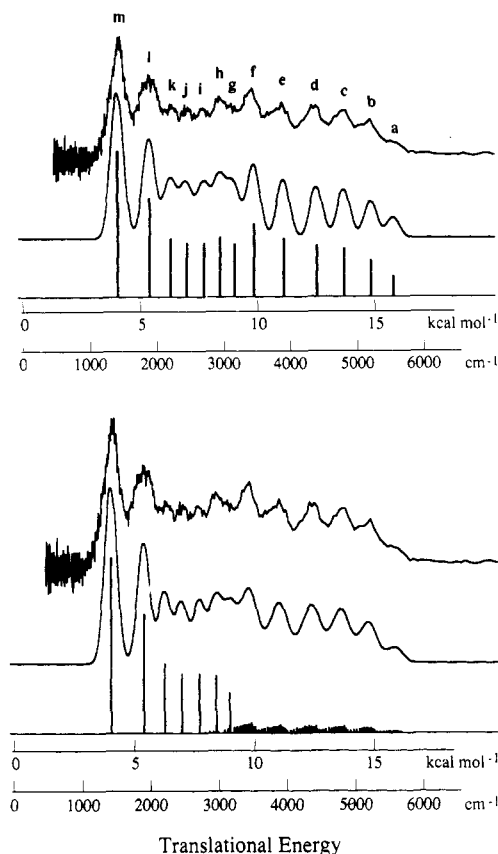
(29) Urdahl, R. S.; Bao, Y.; Jackson, W. M. *Chem. Phys. Lett.*, submitted.

Figure 3. (a) Comparison between data and a stick spectrum convoluted with a 210-cm^{-1} fwhm Gaussian "instrument function". (b) Comparison between data and a "stick-and-Boltzmann" spectrum convoluted with a 210-cm^{-1} Gaussian instrument function. In b, the sticks used to simulate peaks a–f were replaced with 300 K Boltzmann distributions. See text for details.

TABLE I: Parameters for Stick Spectrum Associated with Figure 3a

peak	CM translational energy[a] kcal mol^{-1}	CM translational energy[a] cm^{-1}	rel intensity	energy below peak a (cm^{-1})[b]
a	15.8	5530	0.14	0
b	14.8	5180	0.25	350
c	13.7	4790	0.33	740
d	12.6	4410	0.35	1120
e	11.2	3920	0.40	1610
f	9.9	3460	0.50	2070
g	9.1	3180	0.36	2350
h	8.5	2970	0.41	2560
i	7.8	2730	0.37	2800
j	7.1	2480	0.37	3050
k	6.4	2240	0.40	3290
l	5.5	1920	0.68	3610
m	4.1	1430	1.00	4100

[a] Estimated absolute uncertainty ±0.3 kcal mol^{-1} (±100 cm^{-1}). [b] Estimated relative uncertainty ±50 cm^{-1}.

quently, we also simulated the data using rotational distributions for the a–f peaks, as shown in Figure 3b and listed in Table II. The distributions were chosen ad hoc, but some degree of rotational excitation was necessary in order to obtain the improved fit of Figure 3b relative to 3a.

The relative energies of the "origins" (i.e., $J = 0$ levels listed in Table II) used to simulate the a–f features can be fit by using a ν_2 frequency of 420 cm^{-1}, as shown in Figure 4. Given the present low resolution, anharmonicity is ignored. The corresponding plot of "stick spectrum" values from Table I is similar, with a slightly lower frequency, 410 cm^{-1}. The apparent g/h doublet ~ 3000 cm^{-1} can be included as the sixth member of the progression by averaging the frequencies of the sticks used to simulate the two peaks. Interestingly, if one assumes that l and

TABLE II: Parameters for Spectrum Associated with Figure 3b

peak	CM translational energy[a]		rel intensity	energy below peak a (cm^{-1})[b,c]
	kcal mol^{-1}	cm^{-1}		
a	16.1[c]	5630[c]	0.0436[c]	0[c]
b	15.0[c]	5250[c]	0.0106[c]	380[c]
c	13.9[c]	4860[c]	0.0132[c]	770[c]
d	12.7[c]	4440[c]	0.0140[c]	1190[c]
e	11.3[c]	3950[c]	0.0149[c]	1680[c]
f	10.1[c]	3530[c]	0.0186[c]	2100[c]
g	9.0	3150	0.23	2480
h	8.5	2970	0.33	2660
i	7.8	2730	0.34	2900
j	7.1	2480	0.34	3150
k	6.4	2240	0.40	3390
l	5.5	1920	0.68	3710
m	4.1	1430	1.00	4200

[a] Estimated absolute uncertainty ±0.3 kcal mol^{-1} (±100 cm^{-1}). [b] Estimated relative uncertainty ±50 cm^{-1}. [c] Value for the $J = 0$ member of the Boltzmann distribution; see text.
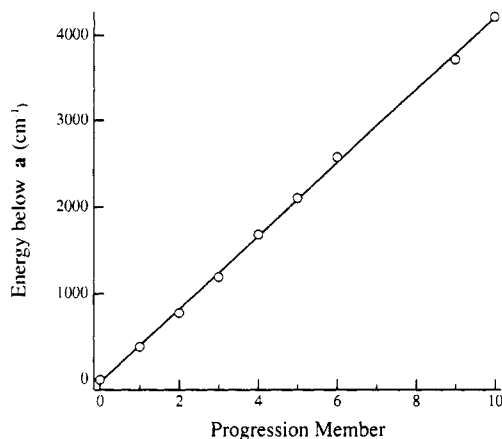

Figure 4. CM translational energy below a (from Table II) vs. progression member: af (origins) are attributed to members 0 to 5, g and h are averaged for 6, while l and m are attributed to 9 and 10. The slope of the straight line is 420 cm^{-1}. Similar results are obtained using energies from Table I.

m are the ninth and tenth members of the progression, they fall on the same straight line as the other points. This suggests that l and m might be attributable to a single progression in the $\tilde{X}^2\Sigma$ state or at least that they are attributable to a bending progression with a similar frequency, i.e., in the $\tilde{A}^2\Pi$ state.

Because of the Π vibronic symmetry of the ν_2 bending mode, it is expected that $\tilde{X}^2\Sigma$ states with odd quanta of ν_2 will interact strongly with the $\tilde{A}^2\Pi$ state.[22] However, there is no evidence of this in the distribution. Similarly, Kanamori and Hirota report observation of a band at 2166 cm^{-1} that they assign to the $\tilde{X}^2\Sigma$-(07^{1}0) upper state.[22] This corresponds to a much smaller ν_2 spacing than we see here. We note that our results are more consistent with an assignment of the observed 2166-cm^{-1} band as $\tilde{X}^2\Sigma(05^10)$.

In addition to C_2H bending, what can explain the other features in the spectrum? In the g–k region ($\sim$2450–3400 cm^{-1} less translational energy than a), the simple pattern seen in a–f is broken, and there are several closely spaced peaks. Of course,

with the present 200-cm^{-1} resolution, many features may simply be unresolved.

As discussed above, $\tilde{A}^2\Pi$ is thought to be 3500–4000 cm^{-1} above $\tilde{X}^2\Sigma$.[17,19–21] Also, it is known that $\tilde{A}^2\Pi$ mixes with nearby $\tilde{X}^2\Sigma$ vibrational levels, and this perturbation has made a definitive assignment of spectral features seen in absorption difficult.[20,21] So where is $\tilde{A}^2\Pi$ in Figure 3? One possibility is that peak a corresponds to $\tilde{X}^2\Sigma(000)$, and peak l derives in whole or part from $\tilde{A}^2\Pi(000)$. It lies $\sim$3600 cm^{-1} above peak a, close to the expected $\tilde{A}^2\Pi$ origin. Also, as noted above, peak l is broader than its neighbors, possibly because of coupling to $\tilde{X}^2\Sigma$ vibrational levels. If this is the case, peak m, which is 470 cm^{-1} higher in internal energy than l and is the dominant feature in the spectrum, can be assigned to $\tilde{A}^2\Pi(010)$, which was seen in emission by Fletcher and Leone.[17] The peaks i–k would then correspond to $\sim$ 2900–3100 cm^{-1} of C_2H internal energy, and therefore one or more of these peaks might be related to ν_1 CH stretch, which remains unassigned.[21]

Another possibility is that the messy g–k region corresponds to the perturbed $\tilde{A}^2\Pi$ origin. If this is the case, peak a corresponds to $\nu_2 > 0$, and D_0 is less than 131.8 kcal mol^{-1}.

From conservation of energy, it is possible, at least in principle, to deduce D_0 from knowledge of the CM translational energy distribution:

$$h\nu - D_0(C_2H-H) = E_{internal}(C_2H) + E_{CM} \qquad (2)$$

where it is assumed that C_2H_2 has negligible internal energy because of expansion cooling. The highest E_{CM} feature that we assign to C_2H_2 photodissociation appears at 16.1 ± 0.5 kcal mol^{-1} (5630 ± 170 cm^{-1}), as shown in Table II. If this corresponds to ground vibronic state C_2H, then $D_0 = 131.8 ± 0.5$ kcal mol^{-1}. This value is in good agreement with other determinations, both experimental and theoretical.[4–6,8] As mentioned above, it appears that the lower value inferred from Doppler-shift measurements can be explained by C_2H photolysis.

This measurement, like others,[4–7] gives only an upper bound to D_0. If the C_2H fragment is formed in its ground vibrational level, then the measurement yields D_0 directly, but if not, the energy of the *lowest occupied level* must be subtracted from the upper bound in order to get D_0. What is the likelihood of the lowest state being unoccupied? In our opinion, one should not dismiss this possibility too quickly. There is a monotonic increase in population for C_2H levels having bending excitation, and there is no a priori reason to believe that peak a corresponds to $v_2 = 0$. These peaks are part of a progression that gains intensity from a to d, and it is possible that the lowest members of the ν_2 progression are simply absent. Thus, the lowest observed level might correspond to $v_2 \geq 1$, in which case the 131.8 kcal mol^{-1} number must be reduced by the energy of the lowest occupied bending level. If this were the case, the $\tilde{A}^2\Pi(000)$ state might lie in the g–k region. Because of this ambiguity, it is not possible to establish D_0 solely on the basis of the present measurements. However, with straightforward experimental improvements, we anticipate close to an order of magnitude improvement in resolution.